X-553-72-148

PREPRINT

DYNAMIC MASS MODELING AND GEOPHYSICAL ANALYSIS OF LUNAR MARIA BASED ON APOLLO TRACKING DATA*

WILLIAM E. STRANGE
MARK L. SANDSON
JAMES P. MURPHY

MAY 1972

GSFC — GODDARD SPACE FLIGHT CENTER —
GREENBELT, MARYLAND

*PRESENTED IN PART AT THE FALL MEETING OF THE AMERICAN GEOPHYSICAL UNION, DECEMBER 6-9, 1971, SAN FRANCISCO, CALIFORNIA

DYNAMIC MASS MODELING AND GEOPHYSICAL ANALYSIS OF LUNAR MARIA BASED ON APOLLO TRACKING DATA*

by

William E. Strange

Mark L. Sandson

Computer Sciences Corporation

and

James P. Murphy

Geodynamics Branch

Goddard Space Flight Center

May 1972

*Presented in part at the Fall Meeting of the American Geophysical Union, December 6-9, 1971, San Francisco, California.

GODDARD SPACE FLIGHT CENTER

Greenbelt, Maryland

CONTENTS

ILLUSTRATIONS

ILLUSTRATIONS (Continued)

TABLES

DYNAMIC MASS MODELING AND GEOPHYSICAL ANALYSIS OF LUNAR MARIA BASED ON APOLLO TRACKING DATA

INTRODUCTION

The first discovery of lunar mass concentrations or mascons associated with the five principle ringed maria on the lunar front side (Muller and Sjogren, 1968) was determined from analysis of the range-rate residuals relative to orbits computed for the nearly polar orbits of Lunar Orbiter 5. The orbit of Lunar Orbiter 5 had a perigee of 100 km and an apogee of 1500 km. This initial analysis was carried out by direct examination of line-of-sight range rate residuals. Because the observed residuals were line-of-sight rather than radial and because of possible distortions in the least squares fitting process, it was recognized that the best method of analysis would be to model the anomalous masses during the orbit differential correction process. Early modeling of this type was carried out by Sjogren et al in 1969 using point masses (Sjogren et al, 1971).

One of the latest refinements (Wong, et al, 1971) involved the simultaneous solution for the masses of 600 circular discs distributed in a regular fashion over the surface of the entire frontside of the moon. In that work data from all five Lunar Orbiter missions, which included both polar and low inclination orbits, as well as some data (about 4.5% of total) from the moderately inclined,

retrograde orbits of Apollo 8 and 12 were used. All of the spacecraft used in that analysis had perilune heights ranging from 54 to 175 km.

A number of interpretations have been made of the various solutions in terms of density distribution and significance relative to mare formation and lunar structure. (Wise and Yates, 1970; Gilvarry, 1970; Conel and Holstrom, 1968; Mason, 1971; Booker, et al 1970.) The difficulty of arriving at definitive conclusions and the wide ambiguity possible due to the non-uniqueness of gravity interpretation was well pointed out by Kane (1969). The ambiguity is greatly increased because of the 100 km and greater altitude of the spacecraft above the lunar surface.

Recently range-rate data have been obtained from Apollo spacecraft at altitudes of 10 to 75 km above the lunar surface. The first report concerning data of this type was that of Gottlieb, et al (1970) who obtained data from the free flight portion of the Apollo 12 lunar excursion module descent. Since that time improved range-rate tracking of the command modules of Apollo 14 and 15 have been obtained while these spacecraft were orbiting some 10 to 25 km above the lunar surface. Initial reports on the results obtained from Apollo 14 have been made by Sjogren et al (1971, 1972) while initial analyses of a portion of the Apollo 15 data have been made by Phillips and Conel (1971). In all cases these analyses of the Apollo 14 and 15 data consisted of computations of the line-of-sight range-rate residuals to be expected of disk models and comparison of these

residuals with observed line-of-sight residuals. The conclusions from these analyses were that the anomalous masses causing the anomalies at Mare Nectaris and Mare Serenetatis were very near the lunar surface.

Present Analyses

A series of lunar gravity analyses have been carried out at NASA Goddard Space Flight Center using Unified S-band tracking network data obtained from Apollos 8, 10, 11, 12, 14, and 15. Interim results of these analyses have been presented previously in GSFC and contractor in house reports (Murphy and Siry (1969), Felsentreger et al (1969), Murphy et al (1970), Fury et al (1971 a, b), Murphy (1972)) and have been presented in papers at technical meetings (Strange et al, 1971) and, to a limited extent, have appeared in technical journals (Murphy and Siry, 1970), and Murphy et al (1970).

The objective of the present report is to summarize the progress obtained to date in these analyses as it relates to the estimation of lunar mass distributions and their geologic interpretation. It is believed that these analyses will be of interest, not only with regard to their lunar significance but also in terms of the insight which they provide as to the degree to which satellite-to-satellite tracking from high to low satellites can provide information on the internal mass distributions of the earth.

The analyses reported here are of two distinct types. The first type of analysis consists of the use of data from Apollo 8, 10, 11, and 12 at two ranges of high altitude (95 to 115 km and 310 to 315 km) to estimate the total mass associated

with various lunar features employing a point mass assumption. This analysis differed from previously reported analyses in that it utilized (1) exclusively Apollo data, (2) a somewhat different method of estimating mass and (3) an independent computer program.

The second type of data analysis reported consisted of detailed analysis of Apollo 14 tracking data. These analyses differ from those of Sjogren et al (1971) in that mass models in the form of rectangles and circular disks curved to follow the lunar curvature were modeled in the differential correction process. The mass of these rectangles and disks were obtained simultaneously with initial conditions in the same way that Wong et al (1971) differentially corrected for disk models. Also an attempt was made to interpret these Apollo 14 results in context with other available lunar data.

Reduction and Analysis of Apollo 8, 10, 11, and 12 Data

In early Apollo missions (Apollo 8, 10, 11 and 12) there were two basic orbit types. The first two revolutions in each mission were eccentric having apolune and perilune distances of 310 to 315 km and 95 to 115 km above the lunar surface, respectively, with apolune over the lunar frontside. The third and all succeeding orbits were nearly circular at 95 to 110 km above the lunar surface. Owing to the slow lunar rotation rate and the moderate to low inclination of the Apollo orbits, the groundtrack of the first two high orbits and several succeeding low orbits for each spacecraft were nearly identical.

For a typical frontside pass from one of these Apollo missions, from 5 to 8 stations tracked the spacecraft. Range-rate tracking data residuals from computed orbits were the same from all stations tracking a pass and changed very little between adjacent orbits at the same height. The residual pattern for orbits of different heights seemed to differ only in that the variations for the higher orbits had decreased amplitudes. This can be seen from an examination of Figures 1a and 1b and is illustrated in several references (See the GSFC Apollo MSFN Metric Tracking Performance Reports 1969a, b, c, 1970a, 1971a, b, for example). In Figures 1a and 1b the Apollo 10 operational model, R2, (Risdal 1969) was used in the orbit computation.

The slope of the range-rate residuals at any time is a measure of a component of the unmodeled acceleration along the direction of the range vector. Since the maximum value of the acceleration was found to occur at about the same point along the groundtrack for both the high and low orbits, these acceleration maxima can be interpreted as being the result of the presence of an unmodeled mass. If the assumption is made that the mascon is essentially a mass point as far as the effect on an object at about 100 km or greater above the lunar surface, the distance of this mass from the spacecraft is a simple function of the height of the spacecraft above the surface and of the depth of the mass point below the surface. From the orbit determination residual pattern for each station in a one orbit solution, a measure of the maximum acceleration

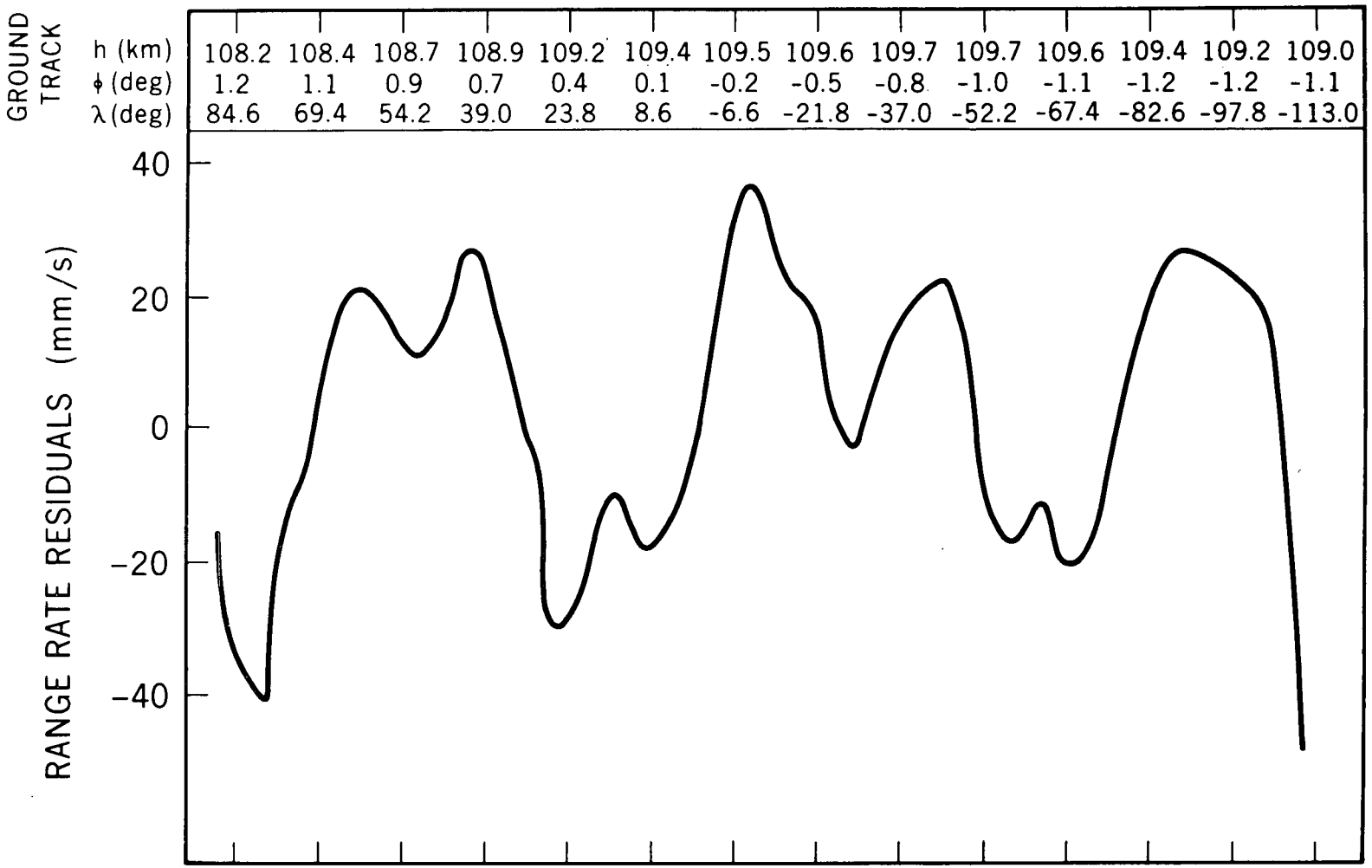

Figure 1a. Apollo 10 Circular (low) Orbit Range Rate Residuals versus Ground Track

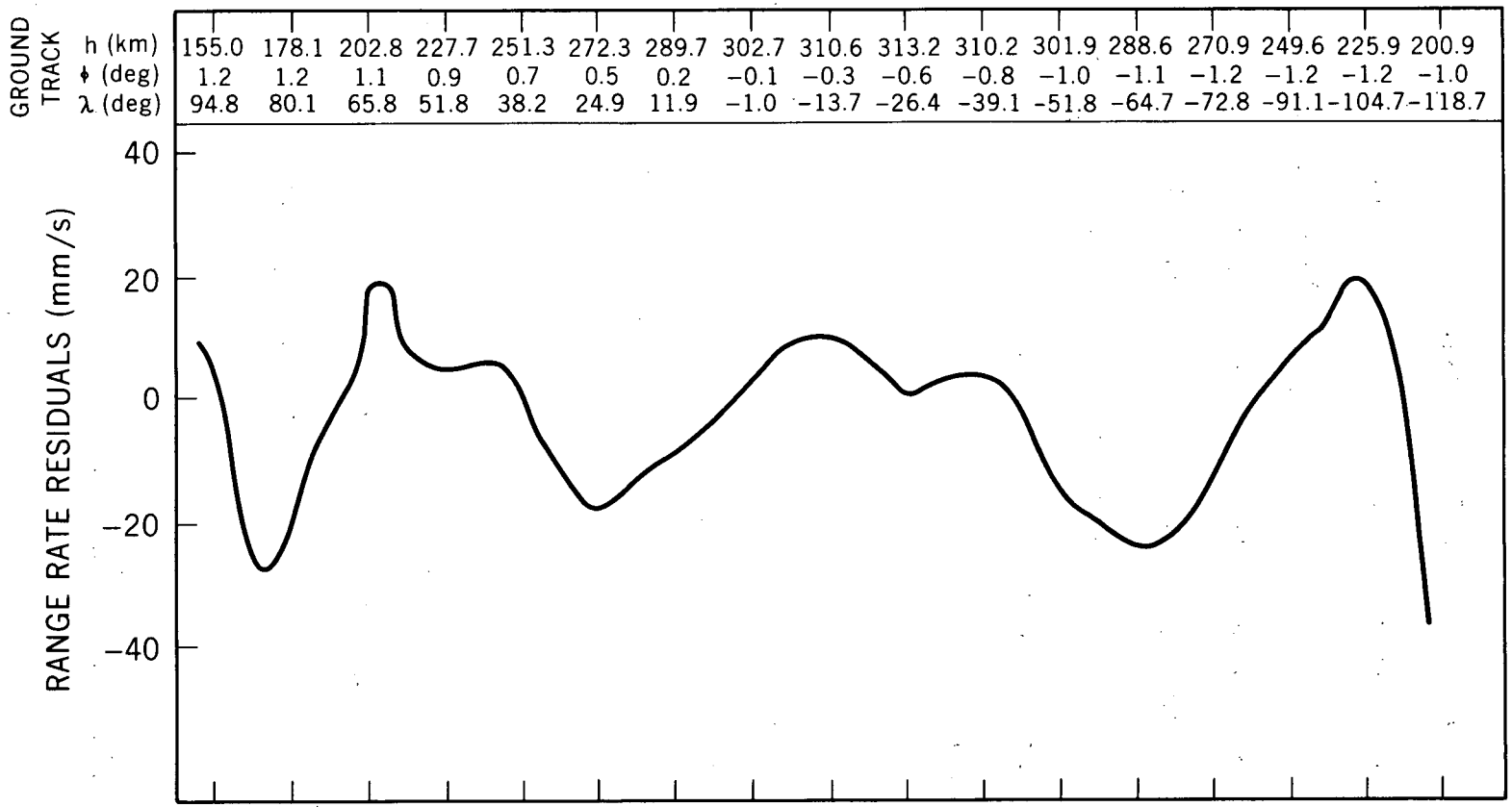

Figure 1b. Apollo 10 Elliptical (high) Orbit Range Rate Residuals versus Ground Track

(an average of the maximum from all stations) can be obtained. This was then done for about four or five consecutive orbits, the first two of which were high, ~ 300 km. Then we have two measurements of the acceleration on the spacecraft at two distinct heights due to a mascon under or nearly under the ground-track. After applying the Newtonian law of gravitation for the residual acceleration twice we have two equations in two unknowns which are easily solved. A set of mass points determined from Apollo orbits together with the missions that were sensitive to them and determination of the same mass points from Lunar Orbiter tracking data are presented in Table 1.

Figure 2 illustrates the improvement to the fit of the tracking data typical for an orbit of Apollo 12 when the last three mascons in Table 1 were added to the operational model, LI (Compton and Tolson 1969). The LI model itself consists only five non-zero coefficients of degree two and three. The addition of the mascons in Table 1 to the operational models for Apollo 11 and 12 also resulted in an improved fit to the tracking data. The root mean square of fit to this data for fifteen orbits of Apollo 11 and 12 was lessened by at least one third and as much as three fifths when the point masses were added to the operational model.

Reduction of Apollo 14 Tracking Data

During reduction of the Apollo 14 data, primary attention was given to the part of the orbit in the vicinity of Mare Nectaris and the crater Theophilus. As shown

Table 1

Mascon Results

Mascon Feature	Apollo Mission	Preliminary Apollo Missions Solution						1970 Lunar Orbiter Solution* Mass 10^{-6} $m_{\mathbb{C}}$
		Transit Height		Mascon Location			Mass 10^{-6} $m_{\mathbb{C}}$	
		high (km)	low (km)	λ(deg)	ϕ(deg)	depth (km)		
Sinus Aestuum**	8	310	112	- 8	10	102	5.2	4.2
Sinus Medii	10	300	109	- 5	0	75	1.4	2.0
Mare Smyth II	11	171	108	85	1	129	7.9	3.1
Mare Nectaris	12	238	116	33	-12	81	7.4	8.4
Oceanus Procellarum	12	308	104	40	5	359	19.9	—

*From Wong et. al., 1971; Mascons were assumed to be on the surface

**From Murphy and Siry, 1970

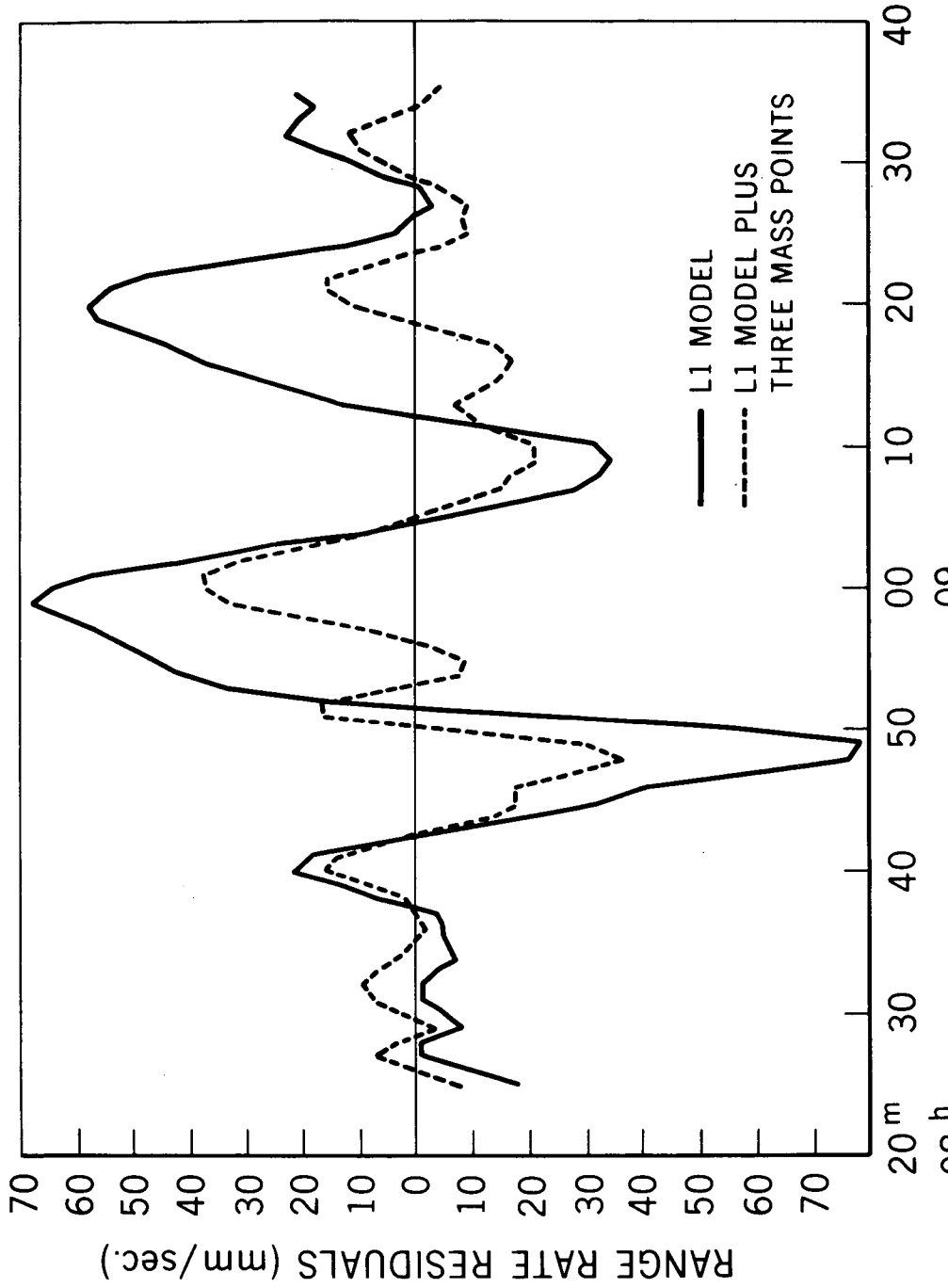

Figure 2. Apollo 12 Orbit 3

by Sjogren et al (1971) and as shown in the profile of Figure 3, the line-of-sight residual accelerations obtained from the Apollo 14 data indicate a gravity positive of ~150 mgal at satellite altitude (~15 km) above Nectaris and a negative acceleration equal to -100 mgal over the Crater Theophilus. Sjogren et al (1971) computed the expected line-of-sight accelerations due to a number of mass disks of varying radii and varying depths below the lunar surface. On the basis of comparison of these computed accelerations with the observed line-of-sight accelerations over Nectaris, Sjogren et al concluded that the Nectaris anomaly could best be explained by a disk of 200 km radius located at the lunar surface. Application to the line-of-sight accelerations of simple approximations commonly used in gravity analysis in exploration geophysics (Grant and West, 1965, pp 282-287) also indicated a shallow origin for the anomalous mass associated with Nectaris and suggested near vertical density contacts.

Directly to the east of the Nectaris positive anomaly the line-of-sight accelerations indicated a negative anomaly equal to ~ -100 mgal in amplitude. It had been demonstrated in simulation experiments that the process of least squares fitting to half revolutions of data to obtain initial conditions could introduce distortion in range rate residuals because of the nature of the least squares process. In particular the creation of spurious gravity negatives adjacent to large gravity positives was shown to be possible. Therefore, the question existed as to the degree to which the ~ 100 mgal negative was real and to what extent it

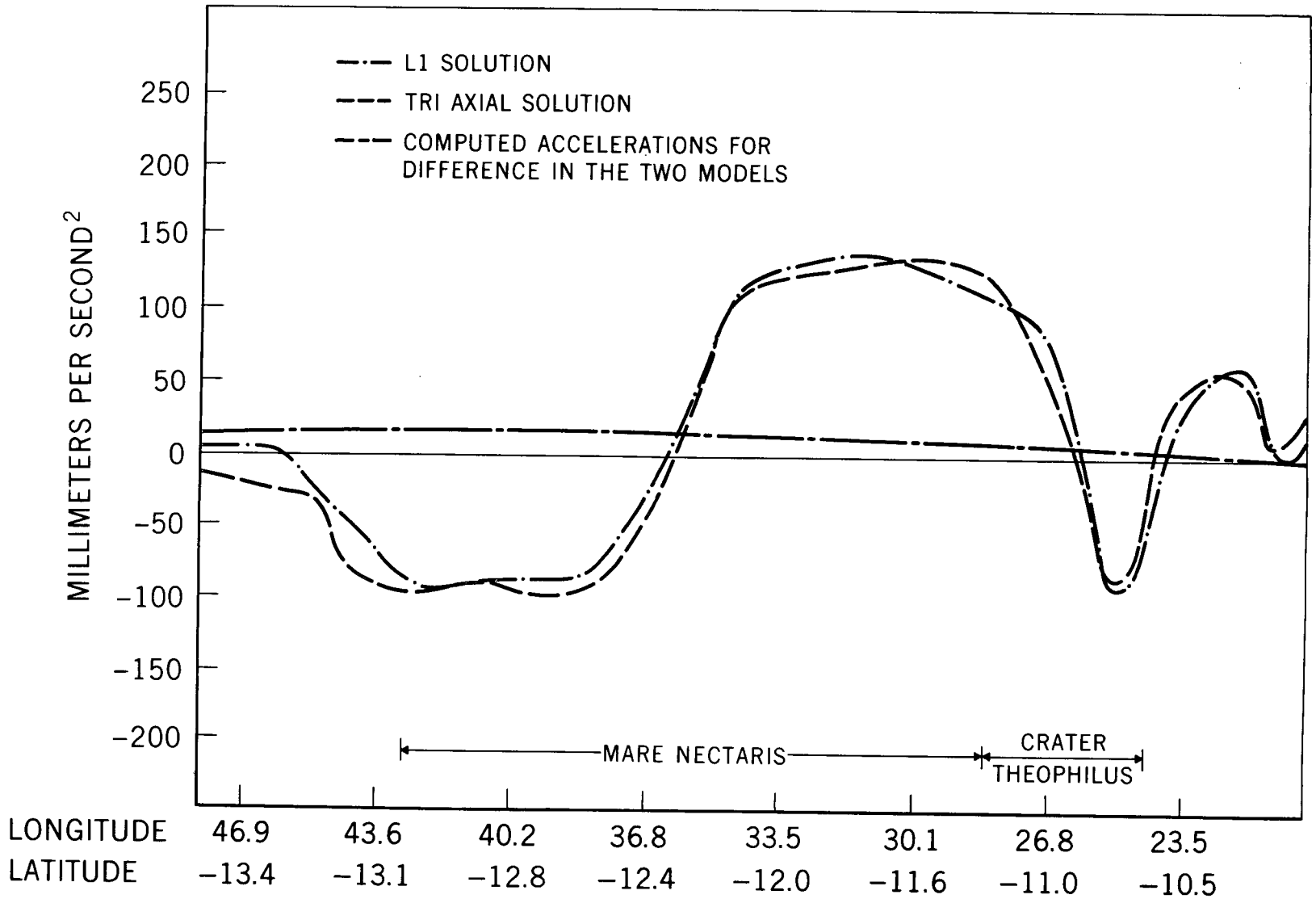

Figure 3. Line of Sight Accelerations in the Vicinity of Mare Nectaris from Complete Frontside Orbit Solutions for 15km High Orbit 3 of Apollo 14

was a result of the least squares fitting process. In order to investigate this question and to improve the interpretation of the Nectaris positive anomaly it was decided to dynamically model mass distributions directly in the differential correction process.

The first test was to model the anomalous mass causing the Nectaris positive gravity anomaly as a mass disk located at a distance of 1735 km from the lunar center and about 15 km below the spacecraft. This disk had its center at selenographic coordinates of 15° S latitude and 35° E longitude and was assigned a radius of 300 km. A differential correction was then carried out with the orbit initial conditions and the mass of the disk computed. Figures 4 and 5 present the line-of-sight velocities before and after modeling the disk for both high and low Apollo 14 orbits. From the residuals, it is clear that, although the mass disk largely accounts for the positive gravity anomaly over Mare Nectaris, it has only minor effect on the gravity negative to the east of Nectaris. It was therefore, concluded that this gravity negative was a real feature of the lunar gravity field.

The next step in data analysis was to model the gravity negative to the east of Nectaris in addition to modeling the Nectaris positive anomaly. In order to assure that the positive and negative masses met at the correct point along the orbit, two mass rectangles were used to represent the positive and negative mass distributions. For a low orbit such as the 15 km high Apollo 14 pass, the

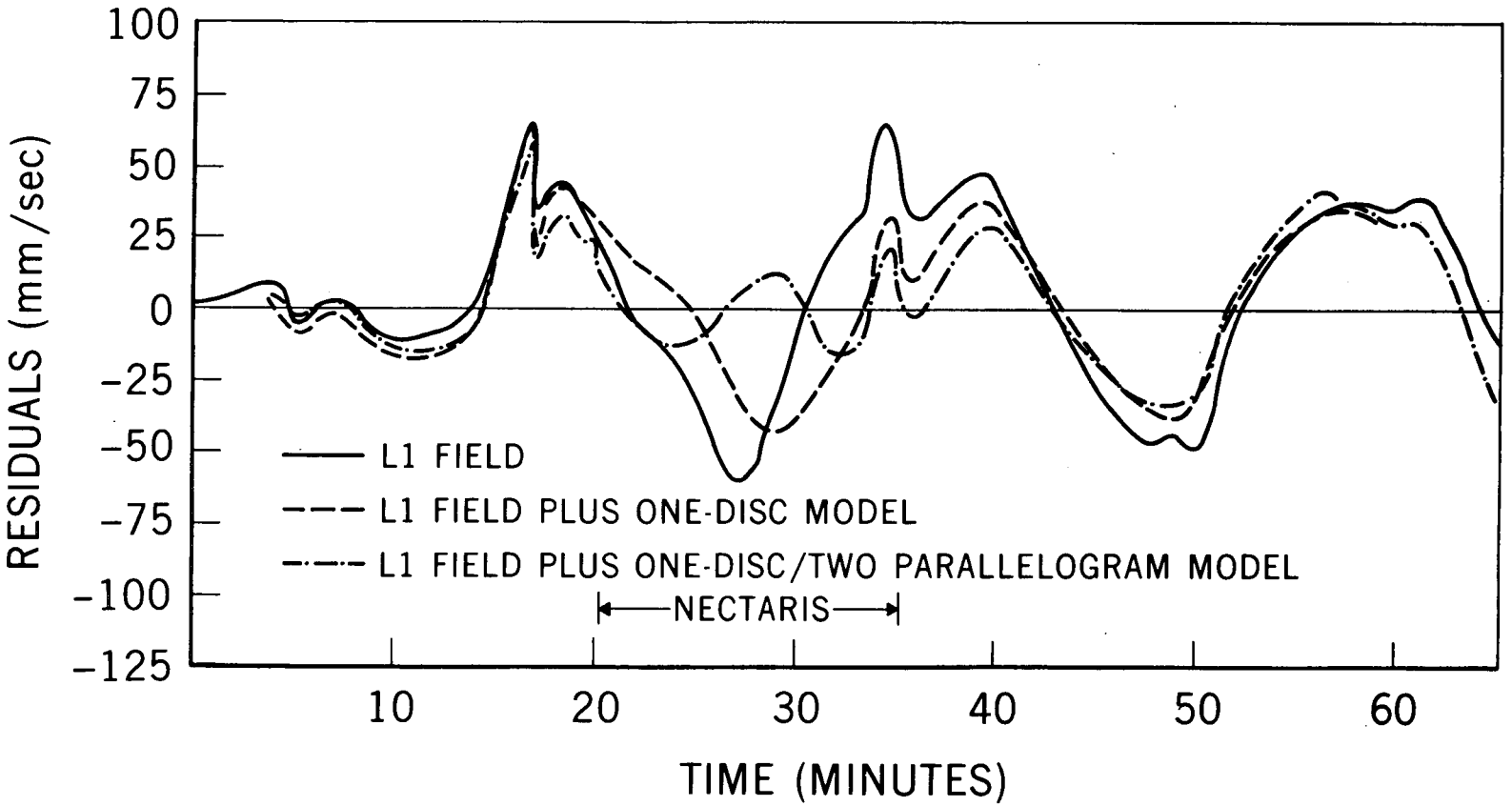

Figure 4. High-Orbit (Revolution 27) Apollo 14 Residuals for Mascon Models

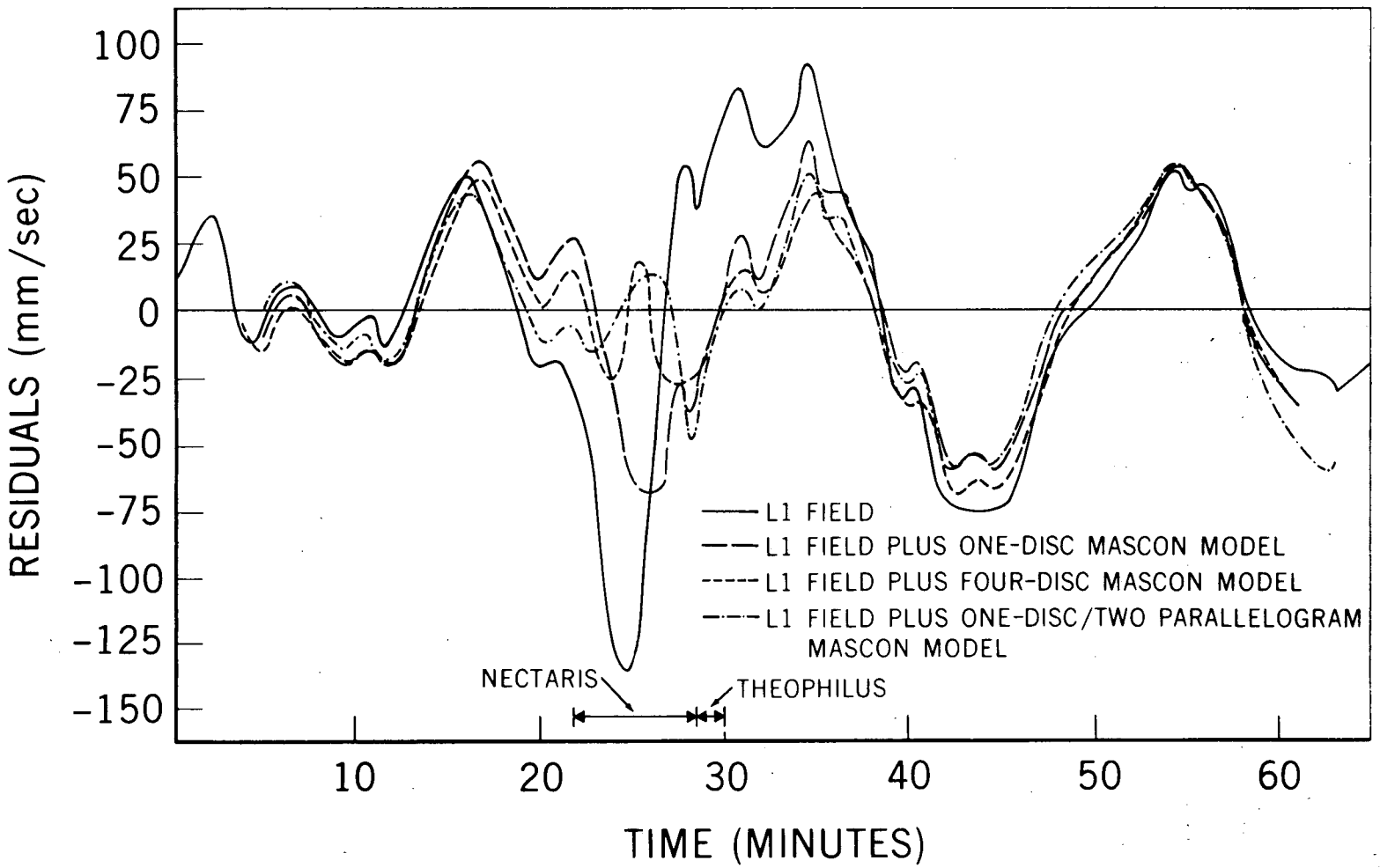

Figure 5. Low-Orbit (Revolution 3) Apollo 14 Residuals for Mascon Models

accuracy of the model within 30 to 50 km on each side of the groundtrack is the key factor. Thus the failure of the rectangle model to match precisely the true horizontal extent of the causative masses is not of great significance. One of the modeled rectangles extended from 29° E to 38° E; the other from 38° E to 44° E. The two rectangles were placed at the lunar surface.

In the differential correction, surface densities of $+5.15 \times 10^5$ gm/cm^2 for the rectangle over Nectaris and -1.62×10^5 gm/cm^2 for the rectangle to the east of Nectaris were obtained. Figure 6 presents a comparison of the observed line-of-sight accelerations and those predicted by the two rectangle model for the vicinity of Nectaris. Further improvements in agreement could have been obtained by experimenting with minor adjustments in the model. The value of such a procedure was felt to be questionable. Any density model found is non-unique. Although other considerations, such as maintenance of physically reasonable density contrasts, allows substantial conclusions as to the general form of the mass causing an observed gravity anomaly, any number of different, equally plausible, small mass variations can be called upon to explain minor differences between the observed gravity and the model gravity.

The most important factor to note is that the rectangular mass layers at the surface accurately map the steep gravity gradients associated with Nectaris. Since the model is equivalent to a vertical contact between positive and negative masses with both masses concentrated at the lunar surface, the chosen model

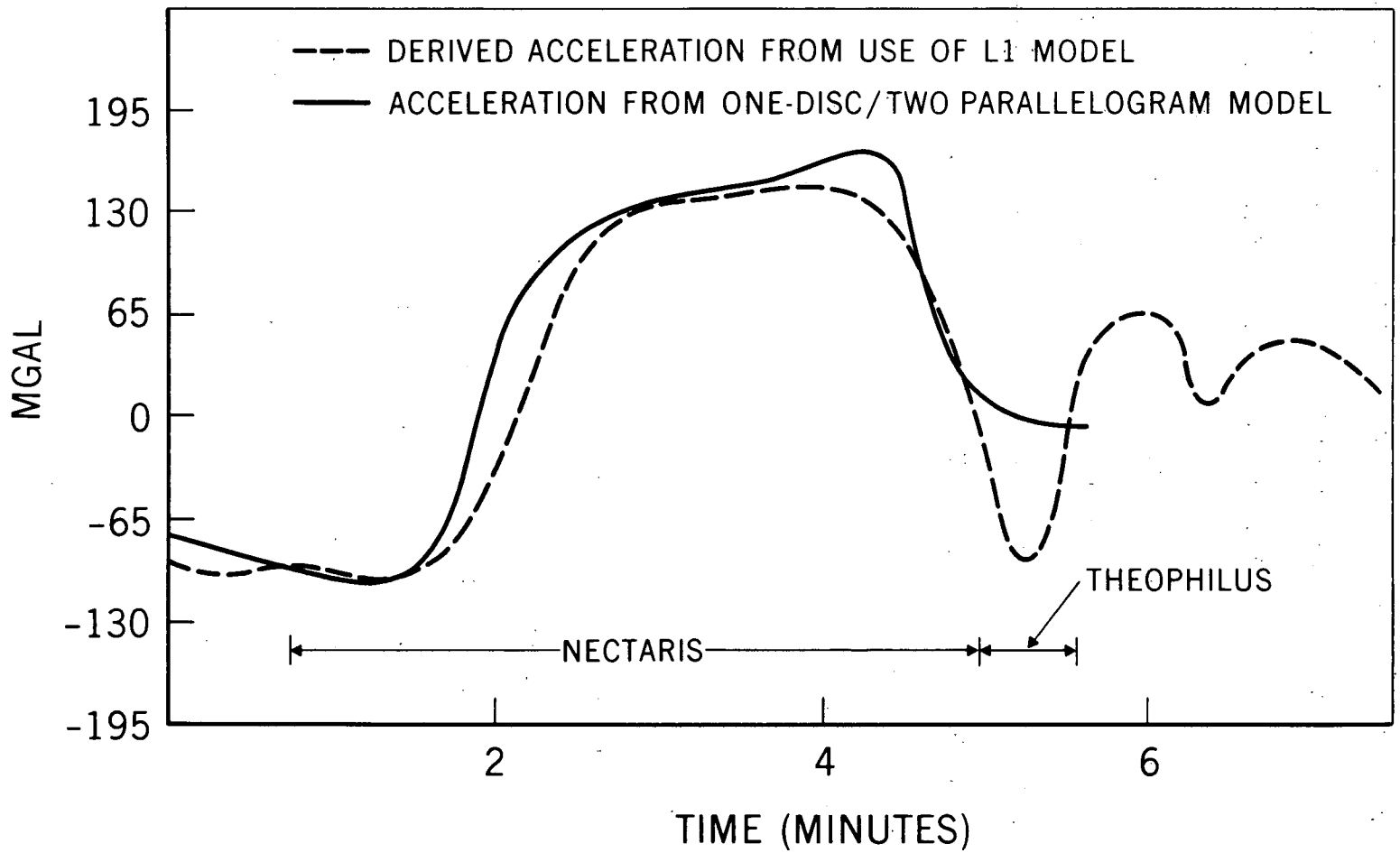

Figure 6. Derived Line-of-Sight Accelerations Produced by One-Disc/Two Parallelogram Mascon Model

provides the steepest possible gravity gradient over the positive-negative mass contact. This leads to the conclusion that mass distributions at depths of greater than 10 to 15 km could not explain the observed gravity anomaly.

In the final solution for the rectangular mass layers, surface densities of 5.15×10^5 gm/cm^2 were found for the positive mass rectangle over Nectaris and -1.62×10^5 gm/cm^2 for the negative mass rectangle east of Nectaris. The actual volume density contrasts that this implies depends upon the vertical extent assumed for the anomalous mass. In making a choice as to the correct vertical extent of the anomalous mass and the implications to be derived from it, it is necessary to consider some basic data concerning the moon and its density distribution.

Numerous analyses have indicated that the moon is very nearly homogenous with a mean density throughout of about 3.35 gm/cm^3. As demonstrated, for example by Kaula (1969), the major topographic variations of the moon are isostatically compensated. If this were not so, there would be gravity variations of over 800 mgal from point to point on the lunar front side due to variations in the attraction of topography. The existence of isostatic compensation implies a differentiated crust of lower density than 3.35 gm/cm^3. Two questions may be asked concerning this low density crust are: What is the density of the material forming it? What is the crustal thickness?

With regard to the first question, both sample analysis and seismic data appear compatible with a crustal density of the order of 2.85 gm/cm^3 (Kanamori, et al, 1969, Sutton, et al, 1970). If 2.85 gm/cm^3 is accepted as the density of the lunar crust, this implies a lunar crust-mantle density contrast of .5 gm/cm^3. With this density contrast, each kilometer of topographic height change would require an isostatic root change of 5.7 km. Since there are elevation changes of approximately 8 km on the lunar front side (Baldwin, 1963, ACIC, 1963-1966), compensation requires a minimum lunar crustal thickness of at least 45 km even if one assumes that, at the lowest point topographically on the front side of the moon, the crustal thickness goes to zero. However, Mare Serenitatis and Mare Imbrium are at low lunar elevations. To explain these anomalies requires that the lunar crust be at least 10 to 20 km thicker than 45 km. This gravimetric computation of a 55 to 65 km lunar crustal thickness appears to be supported by the seismic work of Toksoz, et al (1971) who identify a significant seismic interface at about 65 km depth.

The general lack of correlation between observed acceleration residuals and the topographic gravitational effect characteristic of isostatic compensation is illustrated in Figure 7. Despite the uncertainties in lunar topographic measurements one can conclude from this figure that

1. The gravity anomaly at Nectaris is only slightly related to topography,
2. The gravity negative associated with Theophilus is entirely topographic in origin.

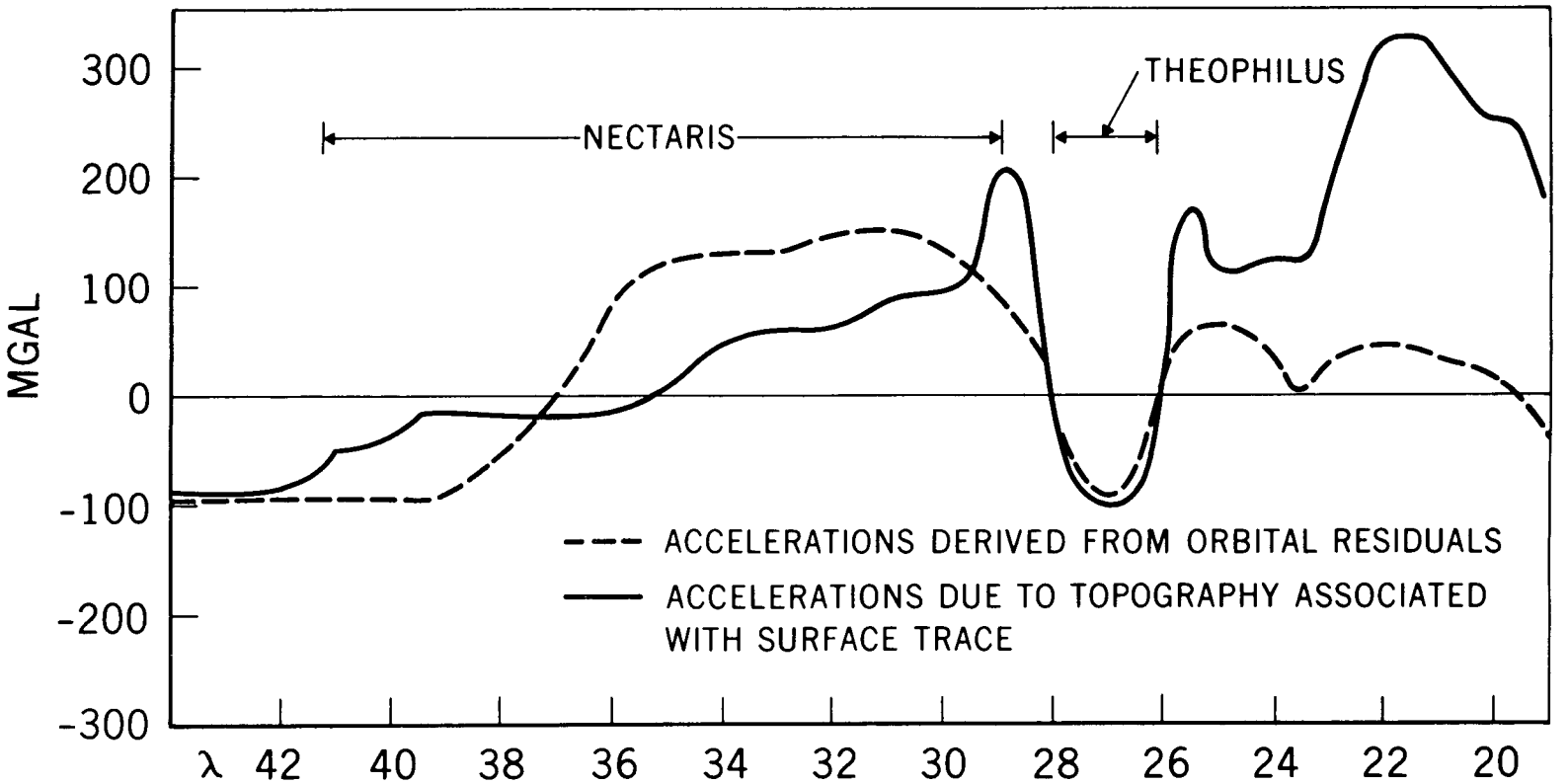

Figure 7. Observed Accelerations vs. Topographical Acceleration Effect for Revolution 3 of Apollo 14

Now consider Mare Nectaris. It must first be pointed out that contrary to the situation with most maria, Mare Nectaris is not a topographic low. Rather, Nectaris lies on a slope between highlands to the west and the low lying Mare Fecuntatis on the east. The areas north and east of Nectaris are at lower elevation than Nectaris. Also assume that the elevation around Nectaris is such that the "normal" crustal thickness (under the assumption of a 65 km maximum crustal thickness) would be about 45 km.

As illustrated in Figure 6, the gravity gradient observed at the eastern edge of Nectaris can be very nearly matched by assuming positive and negative mass density layers at the lunar surface. The physically realistic mass distribution which most closely approximates the physically impossible surface mass layers would be a vertical density contact. In order to match the steep existing gravity gradient at the eastern edge of Nectaris, a nearly vertical density interface close to the lunar surface must be postulated. If the contrast is about 0.65 gm/cm^3, the anomalous density layers would be about 10 km thick. A density contrast of greater than 0.5 gm/cm^3 is supported by the discovery that maria material collected on the Apollo missions has a density of 3.35 gm/cm^3. A smaller assumed density contrast would require thicker anomalous density layers. However, if the density contrast were less than about 0.40 gm/cm^3, a substantial part of the anomalous mass would be at a greater depth than 15 km below the lunar surface. Thus, the steep observed gradient could not be explained.

The density distribution picture obtained from the observed gravity field is therefore one of an excess mass layer over Nectaris extending from the lunar surface to a depth of 10 to 15 km in nearly vertical contact with an area of mass deficiency to the east of Nectaris (this mass deficiency is also very near the surface).

The most interesting aspect of the two facts that:

1. The anomalous mass is within about 15 km of the lunar surface at Nectaris, and
2. The lunar crust at Nectaris appears to be over 40 km thick,

is that these facts are incompatible with the most prominent models used to explain the maria.

To understand the incompatibility that exists, one must recognize an incorrect assumption which is often made. This is the assumption that perfect isostasy implies zero free-air gravity anomalies. For features of finite dimensions (such as the circular lunar maria), this assumption of implied zero free-air gravity anomalies is incorrect.

The manner in which the incorrect assumption leads to erroneous conclusions can be seen in Figure 8. In Figure 8a isostasy would exist if $2.85\ t_1 = 3.35\ t_2$. Consider Figure 8b where additional material of thickness $t_3 = t_1 - t_2$ and density 3.35 gm/cm^3 is added. In one sense, i.e., with respect to the maximum magnitude of the anomaly, it may be proper to say that the gravity anomaly

resulting is that caused by a layer of thickness t_3 and density 3.35 gm/cm^3. In another sense, however, i.e., with respect to the shape of the anomaly, the assumption is incorrect. The gravity anomaly produced by the density distribution of Figure 8b would be that of an anomalous mass t_1 km thick and having a density differential of 0.5 gm/cm^3.

Keeping the above fact in mind, it is clear that the available gravity data at Nectaris is not compatible with the theory of a hole being blasted in a 45 km crust and then being filled up to the beyond isostatic equilibrium, as suggested by Wise and Yates (1970), Rather one is led to a theory illustrated in Figure 9. This figure indicates a condition where a crater some 10 to 15 km deep is formed in a lunar crust of density 2.85 gm/cm^3 and filled with flow material of density 3.35 gm/cm^3. This flow material would presumably be drawn from the lunar mantle through fractures caused at impact. The negative east of Nectaris would arise from fractured crustal material adjacent to the original crater with the fracturing having lowered the crustal density to about 2.65 to 2.70 gm/cm^3.

The model illustrated in Figure 8 appears to fit Serenitatis also as illustrated by the results of Phillips and Conel (1971) and the profile of line-of-sight velocity residuals illustrated in the final MSFN Metric Tracking Report for Apollo 15 (GSFC, 1971). As illustrated in that report large negative anomalies are indicated adjacent to Serenitatis which, based on the analysis of Nectaris described above, can be assumed to be real.

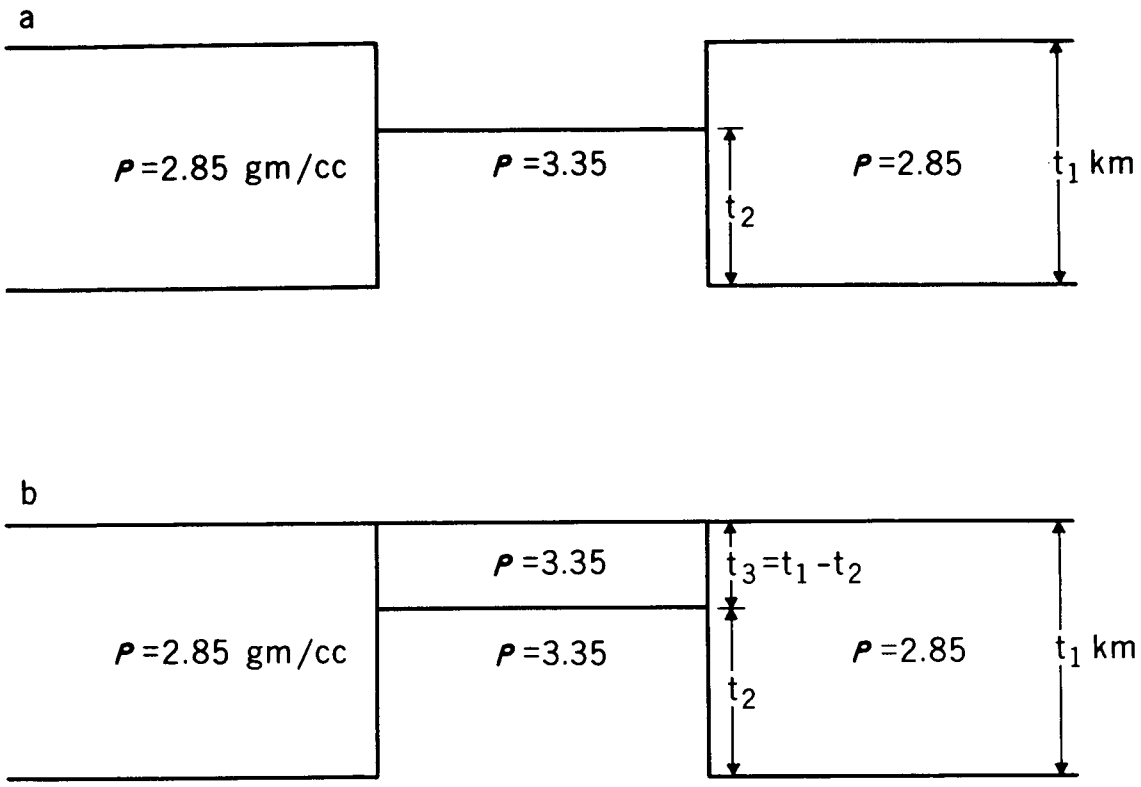

Figure 8. Implications of Incorrect Isostasy Inference

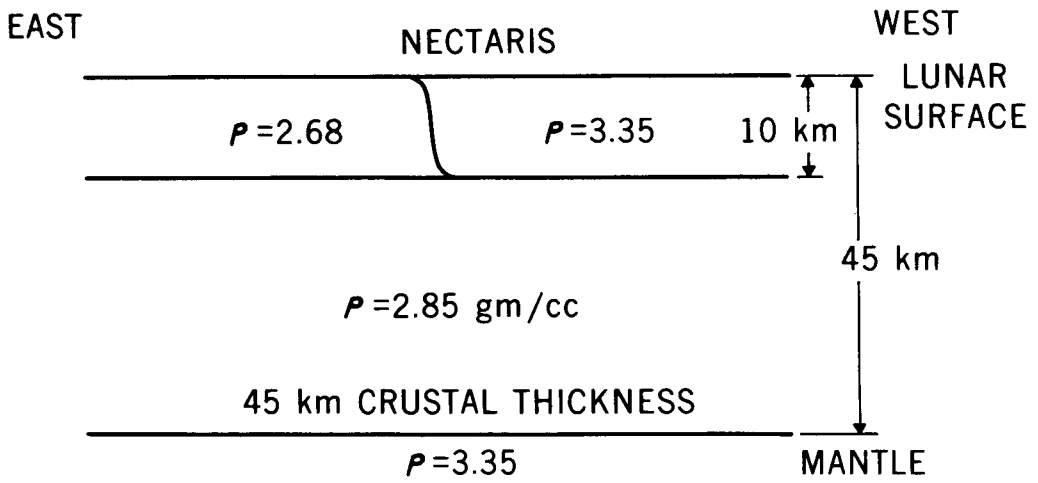

Figure 9. Postulated Density Contrasts at Nectaris

In summary, the gravity field over lunar mascons, as represented by Nectaris and Serenitatis can best be explained by a model such as that of Figure 9. This model implies that the impact of a large body produced a crater some 10 to 15 kilometers deep fracturing the area around and beneath it. Through heating from impact and release of stress lava was formed which flowed up through fractures and filled the craters.

REFERENCES

Baldwin, R. B., "The Measure of the Moon," University of Chicago Press, Chicago, Illinois, 1963.

Booker, J. R., Kovach, R. L., Lu, L., 1970, "Mascons and Lunar Gravity," Journal Geophysical Research, Vol. 75, No. 32, ppg. 6558-6564.

Compton, H. R., and Tolson, R. H. "Study of a Simple Lunar Gravitational Model for Application to Apollo Orbit Determination and Prediction, Langley Research Center Memorandum, June 11, 1969.

Conel, J. E. and Holstrom, G. B., 1968, "Lunar Mascons: A Near Surface Interpretation," Science Vol. 162, No. 3860, pp. 1403-1404.

Felsentreger, T. L., Murphy, J. P., Ryan, J. W., and Salter, L. M., 1969, "Lunar Gravity Field Determined from Apollo 8 Tracking Data," NASA GSFC, Document X-552-69-317, 100 pp.

Fury, R. J., Sandson, M. L., and Strange, W. E., 1971, "Summary of Preliminary Orbit Determination Analysis for Detailed Gravity Field Investigations," CSC Document No. 5035-13800-01 TR., October 1971.

Gilvarry, J. J., 1970, "The Origin and Nature of Lunar Mascons," Radio Science, Vol. 5, page 313.

Gottlieb, P., Muller, P. M., Sjogren, W. L., and Wollenhaupt, W. R., 1971, "Lunar Gravity Over Large Craters from Apollo 12 Tracking Data," Science, Vol. 168, pp. 477-479.

Grant, F. S. and West, G. E., "Interpretation Theory in Applied Geophysics," McGraw-Hill Book Company, New York, 584 pp., 1965.

Kanamori, H., Nur, A., Chung, D., Wones, D., and Simmons, G., "Elastic Wave Velocities of Lunar Samples at High Pressures and Their Geophysical Implications," Science, Vol. 169, No. 3918, pp. 726-727, 1970.

Kaula, W. M., "The Gravitational Field of the Moon," Science, Vol. 166, No. 3913, pp. 1581-1587, 1969.

Kane, M. F., 1969, "Doppler Gravity, A New Method," Journal Geophysical Research, Vol. 74, pp. 6579-6582.

Mason, C. C., 1971, "Nature of the Density Reversal Beneath the Lunar Maria," preprint, paper presented AGU 1971, Fall Meeting, San Francisco, 17 pp.

MSFN Metric Tracking Performance Report Apollo 8/AS-503 Goddard Space Flight Center Report X-832-69-69, February 1969.

MSFN Metric Tracking Performance Report Apollo 10/AS-505 Goddard Space Flight Center Report X-832-69-224, May 1969.

MSFN Metric Tracking Performance Report Apollo 11/AS-506 Goddard Space Flight Center Report X-832-69-367, August 1969.

MSFN Metric Tracking Performance Report Apollo 12/AS-507 Goddard Space Flight Center Report X-832-70-79, March 1970.

MSFN Metric Tracking Performance Report Apollo 14/AS-509 Goddard Space Flight Center Report X-832-71-175, May 1971.

MSFN Metric Tracking Performance Report Apollo 15/AS-510 Goddard Space Flight Center Report X-832-71-434, November 1971.

Muller, P. and Sjogren, W. L., 1968, "Mascons: Lunar Mass Concentrations," Science, Vol. 161, page 680.

Murphy, J. P., Felsentreger, T. L., Wagner, C. A., and Ryan, J. W., 1970, "Lunar Gravity Models for Improved Apollo Orbit Computations," NASA GSFC, Document X-552-70-289, 55 pp. Also, Transactions of the American Geophysical Union Vol. 52, No. 6 (abstract).

Murphy, J. P. and Siry, J. W., 1970, "Lunar Mascon Evidence from Apollo Orbits," Planet, Space Science, Vol. 18, pp. 1137-1141, (also GSFC Document X-550-69-312, July 1969).

Murphy, J. P., 1972, "Mascon Distributions on the Moon," Significant Accomplishments in Science, NASA SP-286, pp. 92-97, 1972.

Phillips, R. J., and Conel, J. E., 1971, "Least Squares Inversion of Lunar Gravity Data," abstract, EOS, Transactions AGU, Vol. 52, No. 11, page 858.

Risdal, R. E., "Development of a Simple Lunar Model for Apollo," Contract Report D2-100819-1, The Boeing Co., Seattle, Washington, 1968.

Ryan, J. W., "The Effect of Mascons on Least Squares Orbit Determination," Internal NASA (GSFC) Memorandum, March 1970.

Sjogren, W. L., Gottlieb, P., Muller, P. M., and Wollenhaupt, W. R., 1971, "Lunar Gravity via Apollo 14 Doppler Radio Tracking," preprint 14th Plenary Meeting of COSPAR, Seattle, 11 pp.

Sjogren, W., Muller, P., Gottlieb, L., Wong, G., Buechler, G., Downs, W., and Prislin, R., 1971, "Lunar Surface Mass Distribution from Dynamical Point Mass Solution," Moon, Vol. 1.

Strange, W. E., Sandson, M. L., Fury, R. J., and Murphy, J. P., 1971, "An Analysis of Continuous Tracking Data for Detailed Gravity Field Determination," Abstract, EOS, Transactions AGU, Vol. 52, No. 11, page 818.

Sutton, G. H., and Duennehier, F. K., "Elastic Properties of the Lunar Surface from Surveyor Spacecraft Data," J. Geophys. Res., Vol. 75, No. 35, pp. 7439-7444, 1970.

Toksoz, M. N., Press, F., Anderson, K., Latham, G., Ewing, M., Dorman, J., Lammlein, D., Sutton, G., Dunnebier, F., and Nakamura, Y., "Internal Structure of the Moon," paper presented 1971 AGU Fall National Meeting, San Francisco, California.

Wise, D. U. and Yates, M. J., 1970, "Mascons as Structural Relief on a Lunar 'Moho'," Journal of Geophysical Research, Vol. 75, No. 2, pp. 261-268.

Wong, L., Buechler, G., Downs, W., Sjogren, W., Muller, P., and Gottlieb, P., 1971, Journal of Geophysical Research, Vol. 76, No. 26, pp. 6220-6236.